



Published in final edited form as:

Eur J Radiol. 2020 February ; 123: 108778. doi:10.1016/j.ejrad.2019.108778.

Radiomic features of the pancreas on CT imaging accurately differentiate functional abdominal pain, recurrent acute pancreatitis, and chronic pancreatitis

Rouzbeh Mashayekhi^a, Vishwa S. Parekh^{a,c}, Mahya Faghih^b, Vikesh K. Singh^b, Michael A. Jacobs^a, Atif Zaheer^{a,b,*}

^aThe Russell H. Morgan Department of Radiology and Radiological Sciences, The Johns Hopkins University School of Medicine, Baltimore, MD, 21205, USA

^bPancreatitis Center, Division of Gastroenterology, Department of Medicine, The Johns Hopkins University School of Medicine, Baltimore, MD, 21205, USA

^cDepartment of Computer Science, The Johns Hopkins University, Baltimore, MD, 21208, USA

Abstract

Purpose: Patients with recurrent abdominal pain and pancreatic enzyme elevations may be diagnosed clinically with recurrent acute pancreatitis (RAP) even with normal imaging or no imaging at all. Since neither abdominal pain nor enzyme elevations are specific for acute pancreatitis (AP), and patients with RAP often have a normal appearing pancreas on CT after resolution of an AP episode, RAP diagnosis can be challenging. This study aims to determine if quantitative radiomic features of the pancreas on CT can differentiate patients with functional abdominal pain, RAP, and chronic pancreatitis (CP).

Method: Contrast enhanced CT abdominal images of adult patients evaluated in a pancreatitis clinic from 2010 to 2018 with the diagnosis of RAP, functional abdominal pain, or CP were retrospectively reviewed. The pancreas was outlined by drawing region of interest (ROI) on images. 54 radiomic features were extracted from each ROI and were compared between the patient groups. A one-vs-one Isomap and Support Vector Machine (IsoSVM) classifier was also trained and tested to classify patients into one of the three diagnostic groups based on their radiomic features.

Results: Among the study's 56 patients, 20 (35.7 %) had RAP, 19 (33.9 %) had functional abdominal pain, and 17 (30.4 %) had CP. On univariate analysis, 11 radiomic features (10 GLCM features and one NGTDM feature) were significantly different between the patient groups. The IsoSVM classifier for prediction of patient diagnosis had an overall accuracy of 82.1 %.

Conclusions: Certain radiomic features on CT imaging can differentiate patients with functional abdominal pain, RAP, and CP.

*Corresponding author at: The Russell H. Morgan Department of Radiology and Radiological Science, Johns Hopkins University, School of Medicine, 601 N. Caroline Street, JHOC 3235 A, Baltimore, MD, 21287, USA. azaheer1@jhmi.edu (A. Zaheer).

Declaration of Competing Interest

Vikesh Singh is a consultant to Abbvie, Ariel Precision Medicine, Orgenesis, and Akcea Therapeutics. Other authors have no disclosures. Other authors have no relevant conflict of interest.

Keywords

Pancreas; Pancreatitis; CT; Abdomen; Radiomics; Recurrent acute pancreatitis; Chronic pancreatitis; Machine learning

1. Introduction

Recurrent acute pancreatitis (RAP) is a clinical condition defined as two or more prior episodes of acute pancreatitis (AP) with near or complete resolution of the disease in-between the episodes. The most common causes include biliary stones or sludge, alcohol consumption, sphincter of Oddi dysfunction, genetic mutations (such as PRSS1 and SPINK1), and anatomic variants of the pancreatic duct interfering with normal flow of pancreatic secretions [1]. 17–22 % of patients diagnosed with AP have recurrence in the future, and up to 36 % of RAP patients eventually advance to chronic pancreatitis (CP) [2,3]. RAP is associated with a lower quality of life and current interventions have not proven to be effective at reducing recurrence [4-6].

Diagnosis of AP can be challenging, such as in the ICU setting, where lack of a proper abdominal examination, non-specific enzyme elevations due to non-pancreatic conditions, and suboptimal non-contrast CT examination may preclude correct diagnosis [7]. When contrast enhanced CT imaging is performed in a patient with AP, it can help assess the severity of disease and helps exclude other causes of acute abdominal pain [8]. However, patients with RAP often have a normal appearing pancreas on CT after resolution of an AP episode and in between recurrent episodes, making the diagnosis of RAP challenging. As a result, patients with normal cross-sectional imaging. This may lead to unnecessary endoscopy or treatment, in patients without actual disease. Therefore, there is a need for diagnostic tools to further corroborate the clinical diagnosis of RAP and to distinguish it from other causes of abdominal pain.

Radiomics is the study of quantitative features of radiologic imaging using texture analysis [9,10] and has shown to provide additional information of underlying pathology in many disease processes such as breast cancer, brain metastasis, and lung cancer [11-14]. We sought to examine radiomic features of the pancreas on CT of patients who presented at our pancreatitis clinic with abdominal pain. These patients underwent a comprehensive clinical examination and were diagnosed with either functional abdominal pain, RAP, or CP. Our primary aim was to determine if radiomic features of the pancreas on CT can differentiate patients with functional abdominal pain, RAP, and CP.

2. Methods

2.1. Study design and data collection

The study was approved by the Johns Hopkins Hospital Institutional Review Board for Human Research and complied with Health Insurance Portability and Accountability Act (HIPPA) regulations. This is a retrospective single center cohort study of adult patients evaluated in pancreatitis clinic at the Johns Hopkins Hospital from 2010 to 2018 by an experienced clinical pancreatologist (VKS). All medical records and imaging studies from

prior AP admissions were obtained and reviewed at our institution. Based on the clinical evaluation, these patients were subsequently categorized into one of the following groups: functional abdominal pain, RAP, or CP.

2.2. Patient selection

All three of the following criteria of the revised Atlanta classification were required for a diagnosis of AP: 1) abdominal pain, 2) abdominal imaging findings consistent with AP, and 3) elevated serum amylase or lipase ≥ 3 times upper limit normal (ULN) [15]. Functional abdominal pain was defined using the ROME IV criteria, with most patients meeting criteria for functional dyspepsia or irritable bowel syndrome [16]. In addition to the ROME IV criteria, we required that all functional abdominal pain patients not have any record of an amylase and/or lipase elevation (≥ 3 times the ULN) to preclude any doubtful diagnosis of RAP to fall into this group. CP was defined according to definite M-ANNHEIM criteria in which one or more of the following features must be present: 1) pancreatic calcification(s); 2) moderate or marked ductal changes per the Cambridge classification using endoscopic retrograde cholangiopancreatography (ERCP) or magnetic resonance cholangiopancreatography (MRCP) if ERCP not performed; 3) marked or persistent exocrine insufficiency defined as pancreatic steatorrhea markedly reduced by pancreatic enzyme supplementation; 4) typical histology from an adequate histological specimen [17].

The exclusion criteria were absence of contrast enhanced abdominal CT, presence of foreign bodies near the pancreas such as stents or surgical clips creating beam hardening artifact on the pancreas, radiological features of AP (including peripancreatic fat stranding, edema and fluid on CT) [18], or prior pancreatic surgery. Of the 225 patients, 169 were excluded based on the exclusion criteria and 56 patients from the cohort met the criteria (Fig. 1). All relevant clinical data including age, sex, race, and body mass index (BMI) was collected from the patient medical records. Alcohol consumption and smoking history were categorized according to definitions utilized in the North American Pancreatitis Study (NAPS2) [19].

2.3. Image acquisition and region of interest

All patients in this study had undergone standard venous phase CT of the abdomen acquired at 60 s post IV contrast injection. Images at our institution were scanned on 64-MDCT scanner (Sensation 64, Siemens Healthineers). Patients were injected with 100–120 mL of iohexol (Omnipaque, GE Healthcare) at an injection rate of 4–5 mL/s. Scanning protocols were customized for each patient to minimize dose but were on the order of 120 kVp, 300 mAs_{eff}, and 0.6–0.8 pitch. The collimation was 64 × 0.6 mm for the 64-MDCT scanner and 128 × 0.6 mm for the dual-source scanner. 3-mm slices were used for the radiomics analysis as these were uniformly available for images across institutions. Only venous phase images were analyzed as they are fairly standard in terms of contrast timing and other phases including pre-contrast and arterial phase images were not included in the analysis due to differences in protocols and acquisition timings of these phases. The imaging protocols and image resolution was fairly standard across most institutions and does not lead to variability in significant Hounsfield differences between studies acquired at different centers. DICOM files of the CT images were downloaded into an in-house MATLAB program to outline the pancreas (segmentation) on every slice using a region of interest (ROI) tool. The

segmentation of the pancreas was manually performed by a 4th year medical student and each slice was double checked by an abdominal radiologist (AZ) with a 10-year experience of reading abdominal CT as an attending for accuracy and if needed modified to ensure that correct anatomy is outlined.

2.4. Radiomic feature extraction

Our MATLAB program extracted 54 radiomic features that fall into five categories (Figs. 2 and 3). These categories are First Order Statistics, Gray Level Co-occurrence Matrix (GLCM), Gray Level Run Length Matrix (GLRLM), Neighborhood Gray Tone Difference Matrix (NGTDM), and morphological features. Each GLCM and GLRLM feature is generated in four different degrees (0° , 45° , 90° , 135°) and an average value is used for these features. We used 64 equally sized bins and gray levels in the analysis. For intra-reader variability measurements, a total of 15 cases (5 from each group) were segmented and radiomic features were extracted at two different times that were three months apart. The Dice Similarity coefficient was calculated between the time points [20].

2.5. Statistical analysis

Wilcoxon rank sum test was used to compare radiomic features of RAP patients with nonspecific abdominal pain patients and CP patients. The radiomic features of nonspecific abdominal pain patients and CP patients were also compared. The individual radiomic feature's predictive performance using the area under curve (AUC) for the receiver operating characteristics (ROC) curve was assessed. All data analysis was performed using Stata/IC 15.1 and MATLAB software program. A p -value of < 0.05 was considered statistically significant.

2.6. Classification

We trained and tested a one-vs-one (OVO) IsoSVM classifier to classify the patients into three groups [11]. The IsoSVM is a hybrid classification algorithm consisting of two algorithms – Isomap and Support Vector Machine (SVM) [21,22]. First, the Isomap algorithm is applied to the high dimensional radiomic feature space to transform it into a lower dimensional linearly separable space. The linear SVM algorithm is then trained on the linearly separable transformed space to classify the dataset into two groups. The IsoSVM algorithm can be extended to classify datasets into multiple groups by training an ensemble of classifiers (OVO IsoSVM) where each classifier is trained to classify between two groups. Our dataset consisted of three groups, which resulted in an ensemble of three IsoSVM classifiers. The optimal classification label for an unseen sample is determined by the classification label that gets the highest number of “+1” predictions.

In the one-vs-one model, there are three binary SVMs learners, with each of them computing a hinge loss. The binary losses are aggregated across all the SVM models using the following equation [23]:

$$\frac{(\sum_{l=1}^L |m_{kl}| g(m_{kl}, s_l))}{\sum_{l=1}^L |m_{kl}|} \quad (1)$$

In this equation, k is the class we are computing the loss for, g is the loss function, which in this case is the hinge loss, s_j is the predicted classification score for the positive class of the SVM model, l , and m is the one-vs-one coding matrix shown below

$$\begin{pmatrix} 1 & 1 & 0 \\ -1 & 0 & 1 \\ 0 & -1 & -1 \end{pmatrix} \quad (2)$$

Each column corresponds to the positive and negative class associated with each trained SVM model. The prediction and ROC curves are computed as follows: for each unknown sample, the class, k that produces the minimum loss using equation above is assigned to that sample. The losses computed for each class corresponding to each sample are used to construct the ROC curves.

2.7. Leave one out cross validation

We evaluated the performance of the OVO IsoSVM classification model using leave-one-out cross validation. For each cross-validation fold, the features used to train the IsoSVM were selected by identifying the features that were significantly different in all three patient group comparisons using Wilcoxon rank-sum test. The IsoSVM model was then trained using the features selected using the aforementioned procedure and tested on the left-out cross validation sample. For consistency, the subset of features used to train the IsoSVM model across multiple cross validation folds was limited to the subset of features that were selected across all the cross-validation folds.

3. Results

Of the 56 patients included in the study cohort, 20 (35.7 %) were diagnosed with RAP, 19 (33.9 %) had functional abdominal pain, and 17 (30.4 %) had CP using the above-described clinical criteria. Compared to RAP and functional abdominal pain patients, CP patients were on average about 10 years older, had a higher incidence of diabetes, and were more likely to be non-white, heavy alcohol drinkers, and current smokers (Table 1).

On univariate analysis, there were 11 radiomic features that were significantly different in all three patient group comparisons (Table 2). Of the 11 features, 10 are GLCM features while one is a NGTDM feature. For these 11 radiomic features, we constructed individual ROC curves to measure the AUC values. The AUC values ranged from 0.77 to 0.95 and 0.73 to 0.92 when comparing RAP patients to nonspecific abdominal pain and CP patients, respectively (Table 3).

The IsoSVM classifier had an overall predictive accuracy of 82.1 %. In one-on-one comparison of the three groups, the nonspecific abdominal pain group had a sensitivity of 79 %, specificity of 100 %, and an AUC of 0.91. The RAP group had a sensitivity of 95 %, specificity of 78 %, and AUC of 0.88 while the CP group's sensitivity and specificity were 71 % and 95 %, respectively, with an AUC of 0.90 (Fig. 4). The intra-variability measurements resulted in a high Dice Similarity coefficient of 91 % (range 86–95 %).

The functional abdominal pain and CP classes had higher misclassification rates (21 % and 29 %, respectively) than the RAP class (5 %). Of the nonspecific abdominal pain patients, three were misclassified as having RAP and one was misclassified as having CP. Only one RAP patient was misclassified to CP while five CP patients were misclassified as having RAP. None of the RAP and CP patients were misclassified as having nonspecific abdominal pain, and the positive predictive value (PPV) for nonspecific abdominal pain was 100 % compared to 85.7 % and 70.4 % for the other two groups.

4. Discussion

We demonstrated, in a cohort of clinically well phenotyped patients, that unique radiomic features on CT can differentiate patients with functional abdominal pain, RAP, and CP. When the OVO ISO-SVM model was used to predict patient diagnosis, the majority of patients were classified into their correct diagnostic group with an overall average accuracy of 82.1 %. Of the patients with a diagnosis of RAP, the model accurately predicted the diagnosis, only based on radiomics, for 19 out of 20 patients. This model did overdiagnosis RAP among all the subjects but the overdiagnosis was mainly due to some of the CP patients being misclassified as RAP. Furthermore, none of the patients with actual disease (RAP and CP) were underdiagnosed as having functional abdominal pain. Therefore, radiomics may be a useful diagnostic aid for patients who present with a diagnosis of RAP based solely on abdominal pain symptoms and laboratory values or unavailability of imaging studies acquired during the AP episode. Differentiation of RAP from other causes of abdominal pain including functional pain using non-invasive means may help prevent overtreatment of patients with invasive measures such as endoscopic ultrasound and ERCP, associated with complications such as AP.

The GLCM features showed the most promise in differentiating between the three entities. Among the individual radiomic features, nine GLCM features and one NGTDM feature were noted to be significant. GLCM features are generated by analyzing the intensity of pairs of voxels in relation to the distance and angle between the paired voxels [10]. We noted that features that were significantly different among these groups related to the measurement of the pancreas homogeneity. Homogeneity 1, homogeneity 2, IMC1, and IMC2 are all features that evaluate homogeneity of the ROI. The nonspecific abdominal pain group consistently had the most homogenous pancreas. Homogeneity 1, homogeneity 2, and IMC1 showed a decrease in pancreas homogeneity in RAP and CP patients, with CP patients having the least homogenous pancreas. Moreover, entropy is a measure of heterogeneity, and it showed the same trend in which CP patients have the most heterogeneous pancreas and nonspecific abdominal pain patients have the least heterogenous pancreas. Patients with functional abdominal pain have no structural changes in their pancreas as the pain is not due to a pancreatic process and their pancreas histology would likely be normal. Therefore, their imaging would be expected to have a more homogenous appearance. Patients with chronic pancreatitis often have anatomical changes such as ductal dilatations and calcifications and their histology would show chronic inflammation and fibrosis. Therefore, we would expect a much more heterogeneous image and our observations are consistent with the definitions. RAP patients have undergone prior acute pancreatitis episodes but have not progressed to a state of chronic pancreatitis. Therefore, it is not surprising that their intensities fall in-

between the two other groups. Among NGTDM features, which analyze the difference between a voxel and its neighboring voxels, contrast was the only significant feature [10]. Contrast quantifies the intensity differences between the neighboring voxels. On average, the nonspecific abdominal pain patients had the lowest contrast while the CP patients had the highest contrast, which is due to the presence of calcific regions in their pancreas.

The features that we found to be significant are in accordance with results from prior radiomic studies that have found GLCM features to be important for textural analysis, with at least three studies showing their significance in distinguishing pancreatic pathology [24-26]. A study of the CT images of 53 patients found that there are 14 GLCM features with individual AUCs ranging from 0.64 to 0.82 that differentiate between high grade and low-grade pancreatic intraductal papillary mucinous neoplasms (IPMN) [24]. When differentiating between pancreatic ductal adenocarcinoma (PDAC) and healthy pancreas tissue, one study of CT slices with visible tumor found GLCM entropy and correlation to be significant [25] while another study examining the entire pancreas on CT found GLCM IMC to be one of its top five maximally relevant features [26]. These previous studies on radiomic features of pancreatic pathology have focused on pancreatic cancers such as IPMN, PDAC, and neuroendocrine tumors [24-28]. There have been very few publications to our knowledge in regards to the radiomic features of HAP or CP. One 2018 study utilized radiomic features to create a predictive model for recurrence of AP among 389 patients admitted for their first AP [29]. They found that their radiomic-based model had a classification accuracy of 87.1 % for their primary cohort and was superior to the clinical model in predicting AP recurrence. However, to our knowledge, no study has differentiated RAP from CP and functional abdominal pain.

This is a preliminary study and it has several limitations. First, we have a relatively small sample with each group consisting of 17–20 patients. Therefore, we were unable to account for factors that affect the pancreas such as age, body mass index, and diabetes. While larger studies need to be conducted to better assess the differences among these groups, these may be prohibitive to conduct since, for example, body mass index as well as the presence, severity, and treatment of diabetes will vary substantially across the population. Second, we did not factor in the onset of initial symptoms to assess the duration of the disease, and did not analyze the total number of AP episodes for our patient population due to the retrospective nature of the study. This would be suitable to conduct in a prospective study to follow the course of patients from the onset of disease symptoms. In our study, we were unable to control for any of these factors due to a relatively small sample size. Finally, patients' CT images were performed both at and outside our institution. The use of different scanners has been shown to lead to variability in the extracted radiomics data particularly in tumor phenotype studies [30-32]. As compared to MRI and ultrasound, CT is found to have higher reproducibility of radiomics analysis due to lesser intrinsic complexity [33,34]. Also, we used similar venous phase images to adjust any variability in contrast timing. Furthermore, our data is relevant to real life medical practice as many patients evaluated for abdominal symptoms in outpatient practice have often had their imaging done at various imaging centers.

In our study, pancreatic segmentation was manually performed to ensure accuracy of our results. However, this is a tedious and lengthy process and there is need for more efficient methods for such an assessment. Automated pancreas localization and segmentation is in a constant state of rapid evolution with machine learning algorithms and has recently shown to perform this task with high accuracy [35]. Furthermore, fully automated segmentation methods for fat [36] quantification have already been applied to measure visceral and subcutaneous fat as well as in the liver for population based steatosis assessment [37]. Similar algorithms may be applied to an abdominal CT acquired for the evaluation of abdominal pain in the instance when differentiation between functional abdominal pain and RAP is sought. Such data may be automatically derived at the time of the patient's visit to the outpatient clinic or at the emergency room and adds further information from already acquired images for differentiating RAP from functional abdominal pain.

In summary, radiomic features may serve as a useful tool in the armamentarium of the gastroenterologists and radiologists for distinguishing patients with functional abdominal pain, RAP, and CP an venous phase CT imaging. Once a more confident diagnosis is established, a careful diagnostic algorithm to identify the etiology of the disease and appropriate therapy may be administered. In clinical practice, it may be challenging to correctly identify the cause of recurrent abdominal pain in patients especially if there are no prior medical records or standard laboratory or radiologic findings leading to more invasive testing. We believe that our preliminary study shows that radiomics offers an additional tool that can potentially be used for diagnostic purposes to extract more information from CT images. Future studies would need to prospectively examine a large number of patients to Identify radiomic values that could be used as potential cutoffs for categorizing individual patients and to predict the course of future disease.

Acknowledgements

Funding was provided in part by the National Institutes of Health (NIH) grant numbers: 5P30CA006973 (Imaging Response Assessment Team-IRAT), U01CA140204, and 1R01CA190299. The Tesla K40s used for this research was donated by the NVIDIA Corporation.

References

- [1]. Testoni PA, Acute recurrent pancreatitis: etiopathogenesis, diagnosis and treatment, *World J. Gastroenterol* 20 (2014) 16891, 10.3748/wjg.v20.i45.16891. [PubMed: 25493002]
- [2]. Sankaran SJ, Xiao AY, Wu LM, Windsor JA, Forsmark CE, Petrov MS, Frequency of progression from acute to chronic pancreatitis and risk factors: a meta-analysis, *Gastroenterology* 149 (2015) 1490–1500, 10.1053/j.gastro.2015.07.066 e1. [PubMed: 26299411]
- [3]. Ahmed Ali U, Issa Y, Hagensnaars JC, Bakker OJ, van Goor H, Nieuwenhuijs VB, Bollen TL, van Ramshorst B, Witteman BJ, Brink MA, Schaapherder AF, Dejong CH, Spanier BWM, Heisterkamp J, van der Harst E, van Eijck CH, Besselink MG, Gooszen HG, van Santvoort HC, Boermeester MA, Risk of recurrent pancreatitis and progression to chronic pancreatitis after a first episode of acute pancreatitis, *Clin. Gastroenterol. Hepatol* 14 (2016) 738–746, 10.1016/j.cgh.2015.12.040. [PubMed: 26772149]
- [4]. Coté GA, Imperiale TF, Schmidt SE, Fogel E, Lehman G, McHenry L, Watkins J, Sherman S, Similar efficacies of biliary, with or without pancreatic, sphincterotomy in treatment of idiopathic recurrent acute pancreatitis, *Gastroenterology* 143 (2012) 1502–1509, 10.1053/j.gastro.2012.09.006 e1. [PubMed: 22982183]

- [5]. Wilcox MC, Seay T, Kim H, Varadarajulu S, Prospective endoscopic ultrasound-based approach to the evaluation of idiopathic pancreatitis: causes, response to therapy, and long-term outcome, *Am. J. Gastroenterol* 111 (2016) 1339–1348, 10.1038/ajg.2016.240. [PubMed: 27325219]
- [6]. Coté GA, Yadav D, Abberbock JA, Whitcomb DC, Sherman S, Sandhu BS, Anderson MA, Lewis MD, Alkaade S, Singh VK, Baillie J, Banks PA, Conwell D, Guda NM, Muniraj T, Tang G, Brand R, Gelrud A, Amann ST, Forsmark CE, Wilcox MC, Slivka A, Gardner TB, Recurrent acute pancreatitis significantly reduces quality of life even in the absence of overt chronic pancreatitis, *Am. J. Gastroenterol* 113 (2018) 906–912, 10.1038/s41395-018-0087-7. [PubMed: 29867178]
- [7]. Muniraj T, Dang S, Pitchumoni CS, Pancreatitis or noT? – Elevated lipase and amylase in ICU patients, *J. Crit. Care* 30 (2015) 1370–1375, 10.1016/j.jcrc.2015.08.020. [PubMed: 26411523]
- [8]. Somogyi L, Martin SP, Venkatesan T, Ulrich CD, Recurrent acute pancreatitis: an algorithmic approach to identification and elimination of inciting factors, *Gastroenterology* 120 (2001) 708–717, 10.1053/gast.2001.22333. [PubMed: 11179245]
- [9]. Lambin P, Rios-Velazquez E, Leijenaar R, Carvalho S, van Stiphout RGPM, Granton P, Zegers CML, Gillies R, Boellard R, Dekker A, Aerts HJWL, Radiomics: Extracting more information from medical images using advanced feature analysis, *Eur. J. Cancer* 48 (2012) 441–446, 10.1016/j.ejca.2011.11.036. [PubMed: 22257792]
- [10]. Parekh V, Jacobs MA, Radiomics: a new application from established techniques, *Expert Rev. Precis. Med. Drug Dev* 1 (2016) 207–226, 10.1080/23808993.2016.1164013. [PubMed: 28042608]
- [11]. Parekh VS, Jacobs MA, Integrated radiomic framework for breast cancer and tumor biology using advanced machine learning and multiparametric MRI, *NPJ Breast Cancer* 3 (2017) 43, 10.1038/s41523-017-0045-3. [PubMed: 29152563]
- [12]. Peng L, Parekh V, Huang P, Lin DD, Sheikh K, Baker B, Kirschbaum T, Silvestri F, Son J, Robinson A, Huang E, Ames H, Grimm J, Chen L, Shen C, Soike M, McTyre E, Redmond K, Lim M, Lee J, Jacobs MA, Kleinberg L, Distinguishing true progression from radionecrosis after stereotactic radiation therapy for brain metastases with machine learning and radiomics, *Int. J. Radiat. Oncol. Biol. Phys* 102 (2018) 1236–1243, 10.1016/j.ijrobp.2018.05.041. [PubMed: 30353872]
- [13]. Press RH, Shu H-KG, Shim H, Mountz JM, Kurland BF, Wahl RL, Jones EF, Hylton NM, Gerstner ER, Nordstrom RJ, Henderson L, Kurdziel KA, Vikram B, Jacobs MA, Holdhoff M, Taylor E, Jaffray DA, Schwartz LH, Mankoff DA, Kinahan PE, Linden HM, Lambin P, Dilling TJ, Rubin DL, Hadjiiski L, Buatti JM, The use of quantitative imaging in radiation oncology: a quantitative imaging network (QIN) perspective, *Int. J. Radiat. Oncol. Biol. Phys* 102 (2018) 1219–1235, 10.1016/j.ijrobp.2018.06.023. [PubMed: 29966725]
- [14]. Parmar C, Leijenaar RTH, Grossmann P, Rios Velazquez E, Bussink J, Rietveld D, Rietbergen MM, Haibe-Kains B, Lambin P, Aerts HJWL, Radiomic feature clusters and Prognostic Signatures specific for Lung and Head & Neck cancer, *Sci. Rep* 5 (2015) 11044, 10.1038/srep11044. [PubMed: 26251068]
- [15]. Banks PA, Bollen TL, Dervenis C, Gooszen HG, Johnson CD, Sarr MG, Tsiotas GG, Vege SS, Classification of acute pancreatitis—2012: revision of the Atlanta classification and definitions by international consensus, *Gut* 62 (2013) 102–111, 10.1136/gutjnl-2012-302779. [PubMed: 23100216]
- [16]. Drossman DA, Hasler WL, Rome IV—functional GI disorders: disorders of gut-brain interaction, *Gastroenterology* 150 (2016) 1257–1261, <https://doi.org/10.1053/j.gastro.2016.03.035>. [PubMed: 27147121]
- [17]. Schneider A, Löhr JM, Singer Mv., The M-ANNHEIM classification of chronic pancreatitis: introduction of a unifying classification system based on a review of previous classifications of the disease, *J. Gastroenterol* 42 (2007) 101–119, 10.1007/s00535-006-1945-4. [PubMed: 17351799]
- [18]. Zaheer A, Singh VK, Qureshi RO, Fishman EK, The revised Atlanta classification for acute pancreatitis: updates in imaging terminology and guidelines, *Abdom. Imaging* 38 (2013) 125–136, <https://doi.org/10.1007/s00261-012-9908-0>. [PubMed: 22584543]

- [19]. Whitcomb DC, Yadav D, Adam S, Hawes RH, Brand RE, Anderson MA, Money ME, Banks PA, Bishop MD, Baillie J, Sherman S, DiSario J, Burton FR, Gardner TB, Amann ST, Gelrud A, Lo SK, DeMeo MT, Steinberg WM, Kochman ML, Etemad B, Forsmark CE, Elinoff B, Greer JB, O'Connell M, Lamb J, Barmada MM, Multicenter approach to recurrent acute and chronic pancreatitis in the United States: the North American pancreatitis study 2 (NAPS2), *Pancreatology* 8 (2008) 520–531, 10.1159/000152001. [PubMed: 18765957]
- [20]. Dice LR, Measures of the amount of ecologic association between species, *Ecology* 26 (1945) 297–302, 10.2307/1932409.
- [21]. Tenenbaum JB, Silva Vd., Langford JC, A global geometric framework for nonlinear dimensionality reduction, *Science* 290 (2000) 2319–2323, 10.1126/science.290.5500.2319. [PubMed: 11125149]
- [22]. Cortes C, Vapnik V, Support-vector networks, *Mach. Learn* 20 (1995) 273–297, 10.1023/A:1022627411411.
- [23]. Allwein E, Schapire R, Singer Y, Reducing multiclass to binary: a unifying approach for margin classifiers, *J. Mach. Learn. Res* 1 (2000) 113–141.
- [24]. Hanania AN, Bantis LE, Feng Z, Wang H, Tamm EP, Katz MH, Maitra A, Koay EJ, Quantitative imaging to evaluate malignant potential of IPMNs, *Oncotarget* 7 (2016), 10.18632/oncotarget.11769.
- [25]. Eilaghi A, Baig S, Zhang Y, Zhang J, Karanicolas P, Gallinger S, Khalvati F, Haider MA, CT texture features are associated with overall survival in pancreatic ductal adenocarcinoma – a quantitative analysis, *BMC Med. Imaging* 17 (2017) 38, 10.1186/s12880-017-0209-5. [PubMed: 28629416]
- [26]. Chu LC, Park S, Kawamoto S, Fouladi DF, Shayesteh S, Zinreich ES, Graves JS, Horton KM, Hruban RH, Yuille AL, Kinzler KW, Vogelstein B, Fishman EK, Utility of CT radiomics features in differentiation of pancreatic ductal adenocarcinoma from normal pancreatic tissue, *Am. J. Roentgenol* 213 (2019) 349–357, 10.2214/AJR.18.20901. [PubMed: 31012758]
- [27]. Canellas R, Burk KS, Parakh A, Sahani Dv., Prediction of pancreatic neuroendocrine tumor grade based on CT features and texture analysis, *Am. J. Roentgenol* 210 (2018) 341–346, 10.2214/AJR.17.18417. [PubMed: 29140113]
- [28]. Permut JB, Choi J, Balarunathan Y, Kim J, Chen D-T, Chen L, Orcutt S, Doepker MP, Gage K, Zhang G, Latifi K, Hoffe S, Jiang K, Coppola D, Centeno BA, Magliocco A, Li Q, Trevino J, Merchant N, Gillies R, Malafa M, on behalf of the F.P. Collaborative, Combining radiomic features with a miRNA classifier may improve prediction of malignant pathology for pancreatic intraductal papillary mucinous neoplasms, *Oncotarget* 7 (2016), 10.18632/oncotarget.11768.
- [29]. Chen Y, Chen T, Wu C, Lin Q, Hu R, Xie C, Zuo H, Wu J, Mu Q, Fu Q, Yang G, Zhang XM, Radiomics model of contrast-enhanced computed tomography for predicting the recurrence of acute pancreatitis, *Eur. Radiol* 29 (2019) 4408–4417, 10.1007/s00330-018-5824-1. [PubMed: 30413966]
- [30]. Zhao B, Tan Y, Tsai W-Y, Qi J, Xie C, Lu L, Schwartz LH, Reproducibility of radiomics for deciphering tumor phenotype with imaging, *Sci. Rep* 6 (2016) 23428, 10.1038/srep23428. [PubMed: 27009765]
- [31]. Lu L, Ehmke RC, Schwartz LH, Zhao B, Assessing agreement between radiomic features computed for multiple CT imaging settings, *PLoS One* 11 (2016) e0166550, 10.1371/journal.pone.0166550. [PubMed: 28033372]
- [32]. Mackin D, Fave X, Zhang L, Fried D, Yang J, Taylor B, Rodriguez-Rivera E, Dodge C, Jones AK, Court L, Measuring computed tomography scanner variability of radiomics features, *Invest. Radiol* 50 (2015) 757–765, 10.1097/RLL.000000000000180. [PubMed: 26115366]
- [33]. Limkin EJ, Sun R, Dercle L, Zacharaki EI, Robert C, Reuzé S, Schernberg A, Paragios N, Deutsch E, Ferté C, Promises and challenges for the implementation of computational medical imaging (radiomics) in oncology, *Ann. Oncol* 28 (2017) 1191–1206, 10.1093/annonc/mdx034. [PubMed: 28168275]
- [34]. Parekh VS, Jacobs MA, MPRAD: a multiparametric radiomics framework, *ArXiv* (2018) 1–32.
- [35]. Roth HR, Lu L, Lay N, Harrison AP, Farag A, Sohn A, Summers RM, Spatial aggregation of holistically-nested convolutional neural networks for automated pancreas localization and

segmentation, *Med. Image Anal* 45 (2018) 94–107, 10.1016/j.media.2018.01.006. [PubMed: 29427897]

- [36]. Lee SJ, Liu J, Yao J, Kanarek A, Summers RM, Pickhardt PJ, Fully automated segmentation and quantification of visceral and subcutaneous fat at abdominal CT: application to a longitudinal adult screening cohort, *Br. J. Radiol* (2018) 20170968, , 10.1259/bjr.20170968. [PubMed: 29557216]
- [37]. Graffy PM, Sandfort V, Summers RM, Pickhardt PJ, Automated liver fat quantification at nonenhanced abdominal CT for population-based steatosis assessment, *Radiology* 293 (2019) 334–342, 10.1148/radiol.2019190512. [PubMed: 31526254]

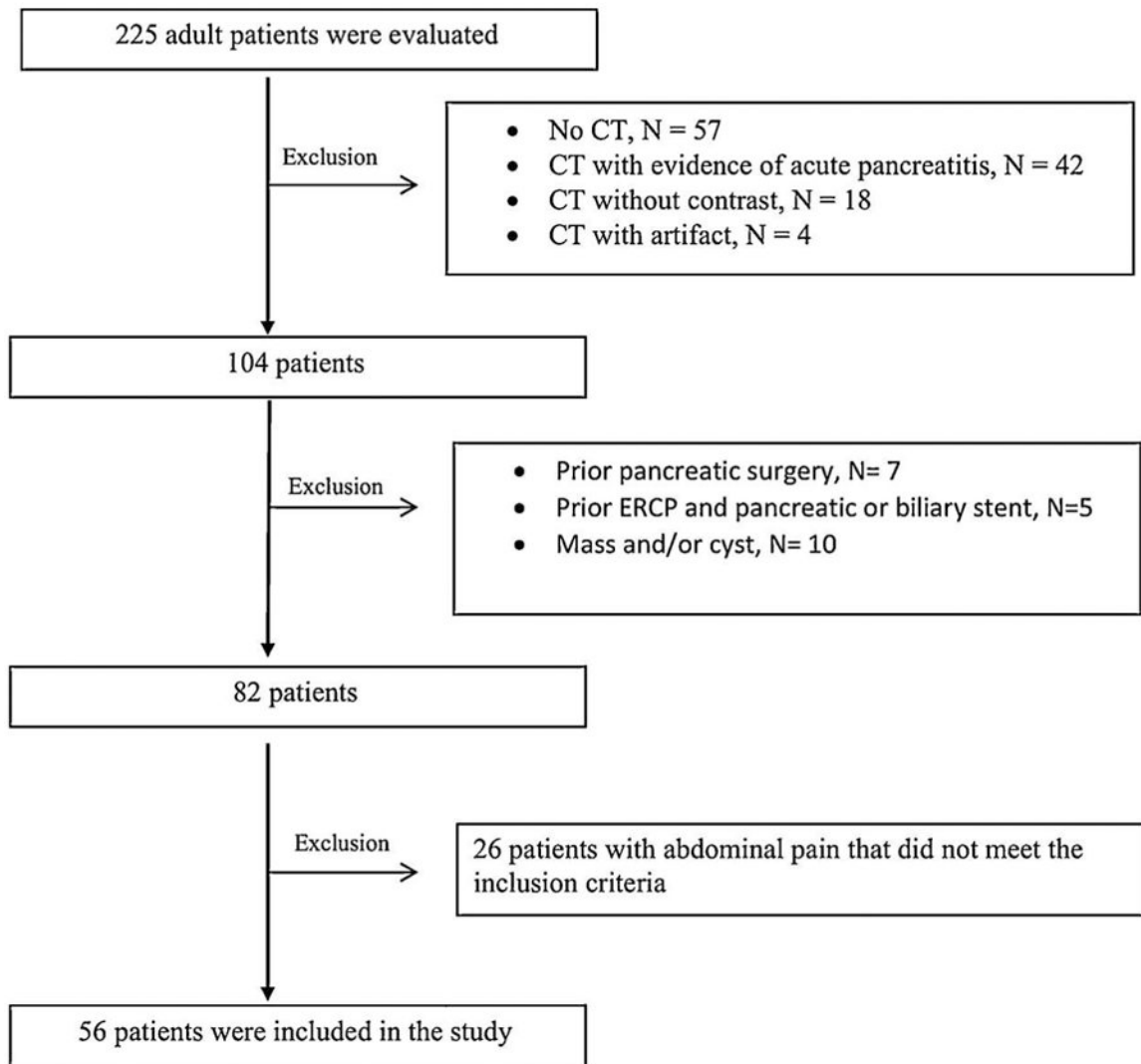


Fig. 1. Sample selection.

Flow diagram demonstrating selection of the study samples.

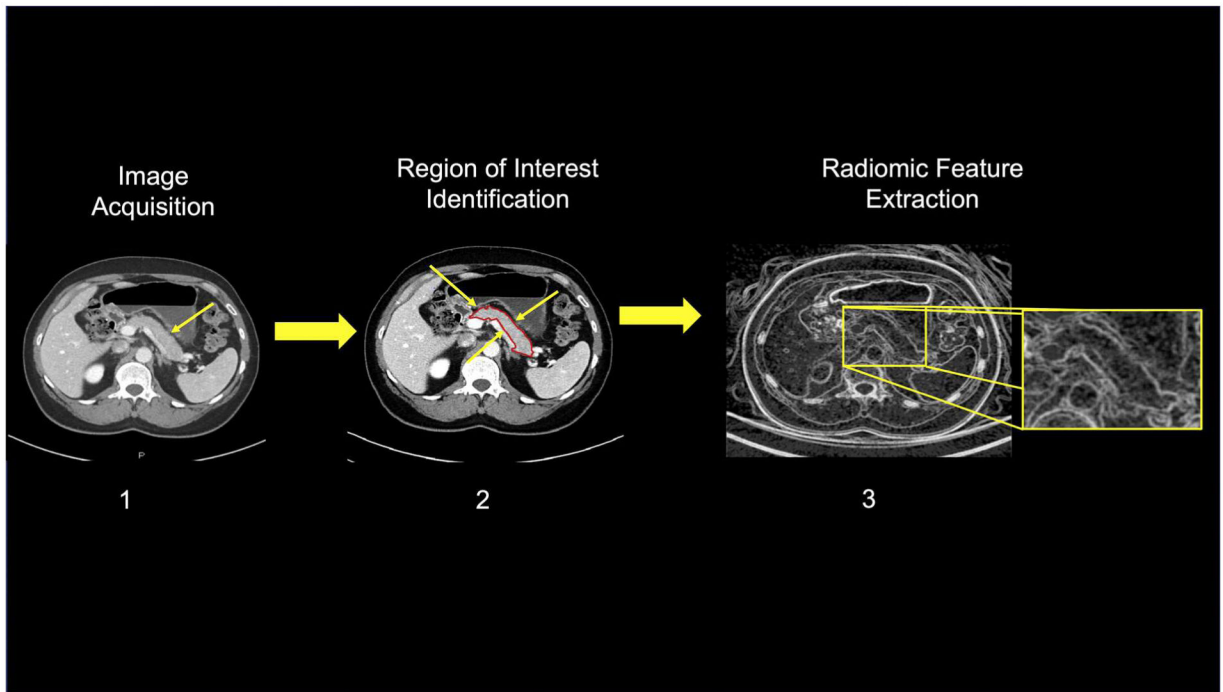


Fig. 2. Image Analysis.

To generate radiomic features, general steps include 1) acquisition of the radiologic images, 2) identification of the regions of interest on the acquired images, 3) extraction of radiomic features from the regions of interests.

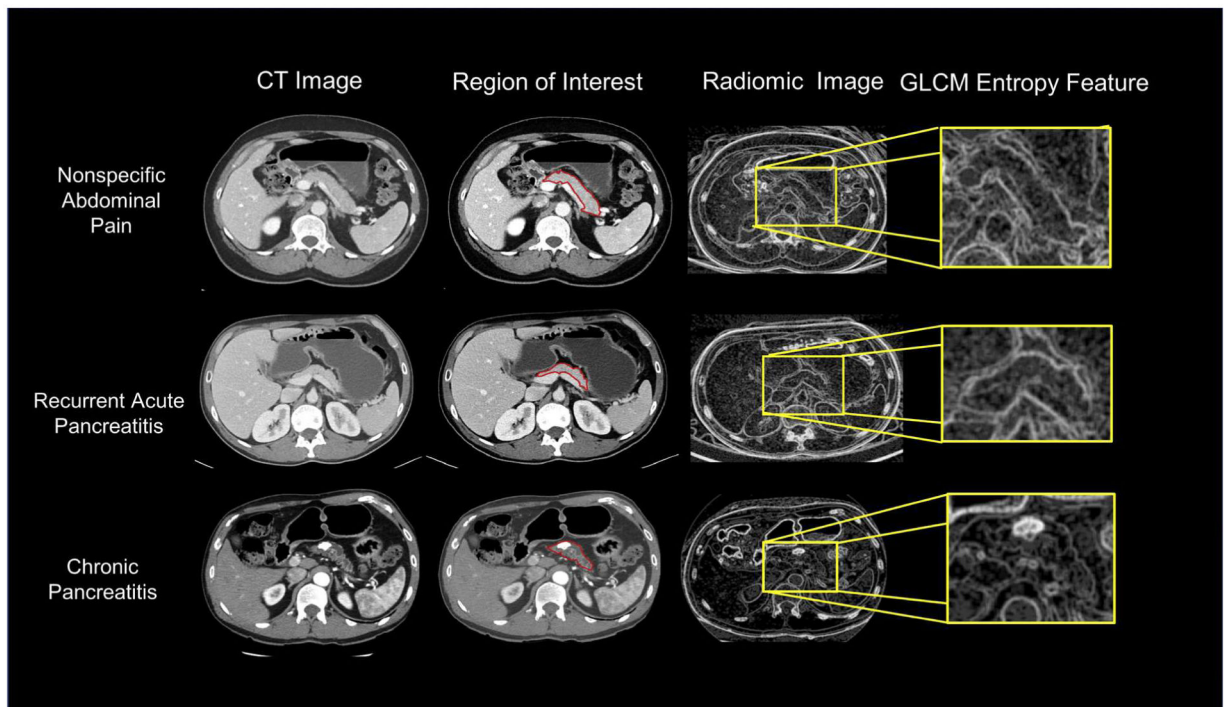


Fig. 3. CT and radiomic sample images based on diagnosis.

For each diagnostic group, each CT slice containing the pancreas (left image) was used to generate the radiomic based image on the right after drawing the region of interest delineating the pancreas (shown with red outline). The radiomic feature in this figure is the GLCM entropy feature, which was found to be significant among all three patient group comparisons.

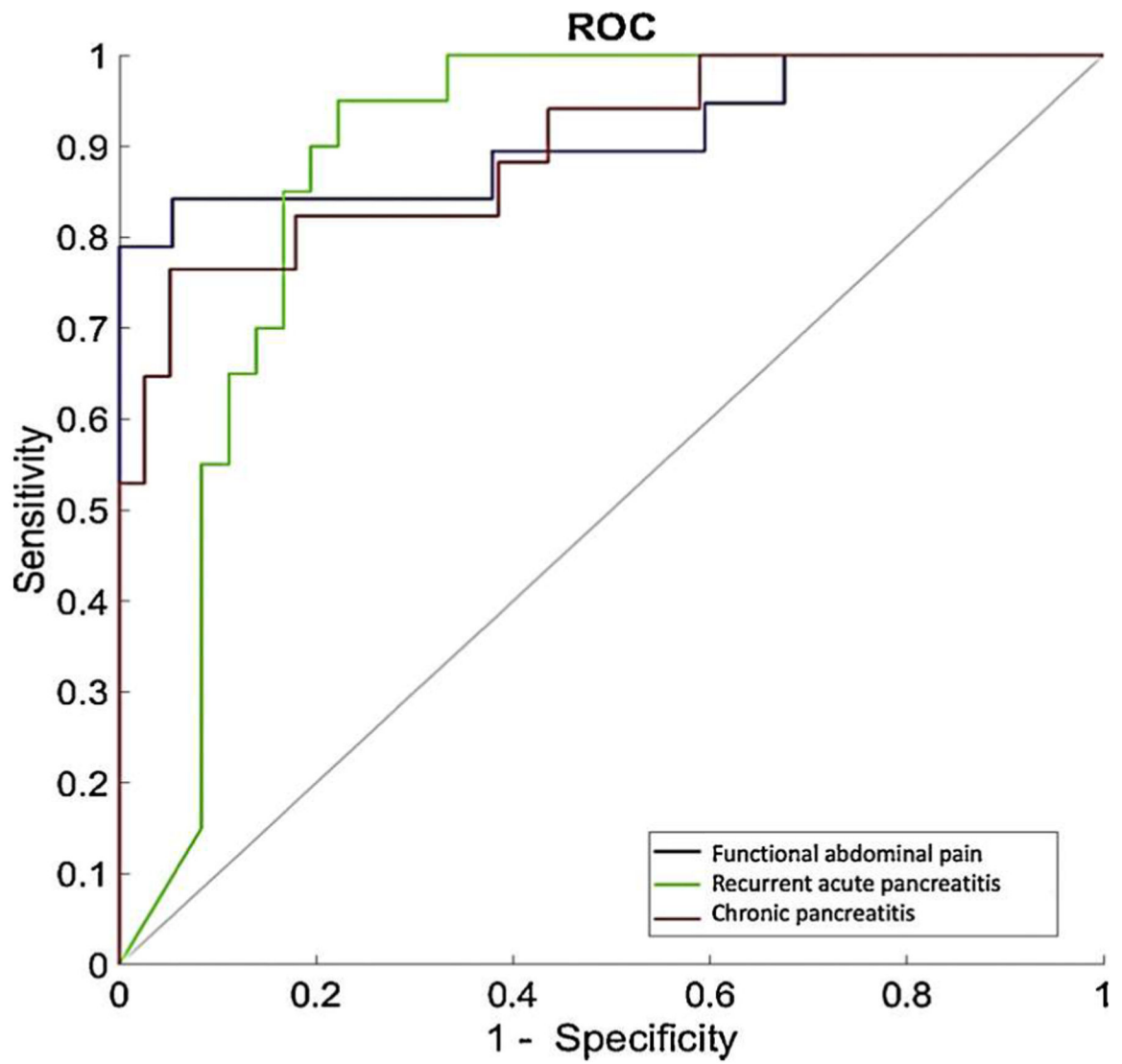


Fig. 4. The Receiver Operating Characteristics Curve for ISO-SVM Model.

Each colored line represents the ROC curves created using the 11 significant radiomic features according to the clinical diagnosis.

Table 1

Baseline characteristics of patients according to clinical diagnosis.

Characteristics	Mean \pm SD or n (%)		
	Functional Abdominal Pain N = 19	Recurrent Acute Pancreatitis N = 20	Chronic Pancreatitis N = 17
Age, years	46.2 \pm 11.3	44.9 \pm 13.7	56.1 \pm 13.4
Sex, male	7 (36.8)	11 (55.0)	9 (52.9)
Race, white	15 (78.9)	17 (85.0)	10 (41.2)
BMI, kg/m ²	25.9 \pm 4.1	23.6 \pm 4.0	22.2 \pm 4.9
Diabetes	2 (10.5)	2 (10.0)	7 (41.2)
Alcohol Use			
Heavy	2 (10.5)	5 (25.0)	8 (47.1)
Moderate	2 (10.5)	1 (5.0)	1 (5.9)
Mild	4 (21.1)	1 (5.0)	1 (5.9)
Abstinent	11 (57.9)	13 (65.0)	7 (41.2)
Smoking History			
Current	2 (10.5)	3 (15.0)	5 (29.4)
Past	2 (10.5)	7 (35.0)	5 (29.4)
Never	15 (78.9)	10 (50.0)	7 (41.2)

Abbreviation: BMI – Body Mass Index.

Table 2

Mean \pm standard deviation of significant radiomic features based on clinical diagnosis.

Radiomic Features	Nonspecific Abdominal Pain	Recurrent Acute Pancreatitis	Chronic Pancreatitis
Cluster Prominence	442.04 \pm 223.23	66.51 \pm 124.04	2.53 $\times 10^4$ \pm 3.91 $\times 10^3$
Cluster Shade	-0.55 \pm 2.19	-3.48 \pm 4.15	549.4 \pm 779.07
Cluster Tendency	1.23 \pm 0.88	1.99 \pm 1.21	27.50 \pm 36.35
Contrast ^a	5.97 $\times 10^{-6}$ \pm 1.29 $\times 10^{-5}$	2.12 $\times 10^{-5}$ \pm 1.05 $\times 10^{-5}$	4.59 $\times 10^{-5}$ \pm 3.09 $\times 10^{-5}$
Correlation	0.26 \pm 0.15	0.57 \pm 0.11	0.70 \pm 0.13
Entropy	0.77 \pm 0.69	1.76 \pm 0.49	2.47 \pm 0.71
Energy	0.42 \pm 0.12	0.29 \pm 0.14	0.19 \pm 0.14
Homogeneity 1	215.56 \pm 117.78	0.82 \pm 0.06	0.76 \pm 0.07
Homogeneity 2	219.45 \pm 119.23	0.82 \pm 0.06	0.75 \pm 0.08
IMC 1	0.24 \pm 0.22	-0.21 \pm 0.06	-0.27 \pm 0.8
IMC 2	0.84 \pm 0.18	0.55 \pm 0.10	0.69 \pm 0.14

Abbreviation: IMC – Informational Measure of Correlation.

^aThis is a Neighborhood Gray Tone Difference Matrix (NGTDM) feature. All other features are Gray Level Co-occurrence Matrix (GLCM) features.

Table 3

AUC and *p*-values of individual radiomic features in one-on-one group comparisons.

Radiomic Features	RAP vs. Functional Abdominal Pain		RAP vs. CP	
	AUC	<i>p</i> -value	AUC	<i>p</i> -value
Cluster Prominence	0.89	< 0.001	0.89	< 0.001
Cluster Shade	0.84	< 0.001	0.92	< 0.001
Cluster tendency	0.77	0.004	0.89	< 0.001
Contrast	0.86	< 0.001	0.75	0.008
Correlation	0.91	< 0.001	0.78	0.008
Energy	0.78	0.003	0.75	0.035
Entropy	0.87	< 0.001	0.82	0.006
Homogeneity 1	0.86	< 0.001	0.73	0.015
Homogeneity 2	0.86	< 0.001	0.74	< 0.048
IMC 1	0.95	< 0.001	0.74	0.008
IMC 2	0.89	< 0.001	0.80	0.009

Abbreviation: IMC – Informational Measure of Correlation; RAP – Recurrent Acute Pancreatitis CP – Chronic Pancreatitis.

Note: *p*-values are based on the Wilcoxon rank sum test.